

# Orbital-Spin Mode-Coupling Theory for $\text{LaFeAsO}_{1-x}\text{H}_x$ : Pnictogen Height Instability and Superconductivity due to Orbital Fluctuations

Seiichiro ONARI<sup>1</sup>, Youichi YAMAKAWA<sup>2</sup>, and Hiroshi KONTANI<sup>2</sup>

<sup>1</sup> *Department of Applied Physics, Nagoya University, Furo-cho, Nagoya 464-8603, Japan.*

<sup>2</sup> *Department of Physics, Nagoya University, Furo-cho, Nagoya 464-8602, Japan.*

(Dated: March 24, 2019)

The isostructural transition in the tetragonal ( $C_4$ ) phase, with sizable change in the As-height, is realized in heavily H-doped  $\text{LaFeAsO}$ , Pr-doped  $\text{CaFe}_2\text{As}_2$ , and Na-doped  $\text{BaFe}_2\text{As}_2$ . Here, we explain the overall phase diagram of  $\text{LaFeAsO}_{1-x}\text{H}_x$  by considering the vertex correction (VC) due to spin fluctuations. In heavily-doped case ( $x \sim 0.5$ ), the non-nematic orbital order is caused by the VC due to  $d_{xy}$ -orbital spin fluctuations, and triggers the  $C_4$  isostructural transition. In lightly-doped case ( $x \sim 0$ ), the orthorhombic phase is realized by the orbital-nematic order, which originates from the VC due to  $(d_{xz}, d_{yz})$ -orbital spin fluctuations. The non-nematic orbital fluctuations that couple to the As-height change would be essential for the second- $T_c$  dome in  $\text{LaFeAsO}_{1-x}\text{H}_x$ .

PACS numbers: 74.70.Xa, 74.20.-z, 74.20.Rp

The normal-state phase diagram of Fe-based superconductors is important to reveal the mechanism of superconductivity and essential electronic states. In many compounds, the structure transition from tetragonal ( $C_4$ ) to orthorhombic ( $C_2$ ) is realized at  $T_S$ , and the antiferromagnetic (AFM) order appears at  $T_N$  below  $T_S$ . The superconductivity is realized near the structural quantum critical point (QCP) at  $T_S = 0$  and/or the magnetic QCP at  $T_N = 0$ . For example, the optimum  $T_c$  in  $\text{FeSe}_x\text{Te}_{1-x}$  is realized near the structural QCP at  $x \approx 0.6$  [1], whereas AFM order is absent for  $x > 0.4$ .

To explain the  $C_2$  structure transition, both the spin-nematic [2] and orbital-nematic [3–6] mechanisms had been proposed. The former predicts that the spin-nematic order ( $\langle \mathbf{s}_A \cdot \mathbf{s}_B \rangle \neq 0$ ) can occur above  $T_N$ , when the magnetism is suppressed ( $\langle \mathbf{s}_{A,B} \rangle = 0$ ) by the  $J_1$ - $J_2$  frustration. As for the latter scenario, orbital-nematic order is induced by spin fluctuations, due to strong orbital-spin mode-coupling described by the vertex correction (VC) [5]. Both mechanisms can explain the shear modulus  $C_{66}$  softening [7, 8]. The orbital mechanism would be consistent with the large  $d$ -level splitting  $E_{yz} - E_{xz} \sim 500\text{K}$  in the  $C_2$  phase [9, 10], and with the large orbital susceptibility given by Raman spectroscopy [11, 12]. Since the superconductivity is realized next to the orbital and spin ordered phase, both fluctuations would be essential for the pairing mechanism.

The unique phase diagram of  $\text{LaFeAsO}_{1-x}\text{H}_x$  with double-dome superconducting phase [13, 14] provides a significant crucial test for existing theories. The second superconducting dome ( $x \geq 0.2$ ) is next to the “ $C_4$  isostructural phase transition” with sizable change in the  $c$ -axis length (or As-height) for  $0.45 < x < 0.5$  [15, 16]. (The  $c$ -axis length is unchanged in the  $C_2$  structure transition at  $x \sim 0$ .) Similarly, high- $T_c$  ( $\sim 50\text{K}$ ) superconductivity is realized near the “collapsed  $C_4$  phase” in Pr-doped  $\text{CaFe}_2\text{As}_2$  [17] and La and P co-doped  $\text{CaFe}_2\text{As}_2$  [18]. These experiments indicate a close relation between

the As-height instability and high- $T_c$  superconductivity. Authors in Ref. [19] discussed that the  $C_4$  phase in  $(\text{Ba},\text{Na})\text{Fe}_2\text{As}_2$  originates from the  $C_4$  magnetic order. However, stripe magnetic order ( $=C_2$  symmetry) is realized in  $\text{LaFeAsO}_{1-x}\text{H}_x$  at  $x \sim 0.5$  [15], indicating small spin-lattice coupling.

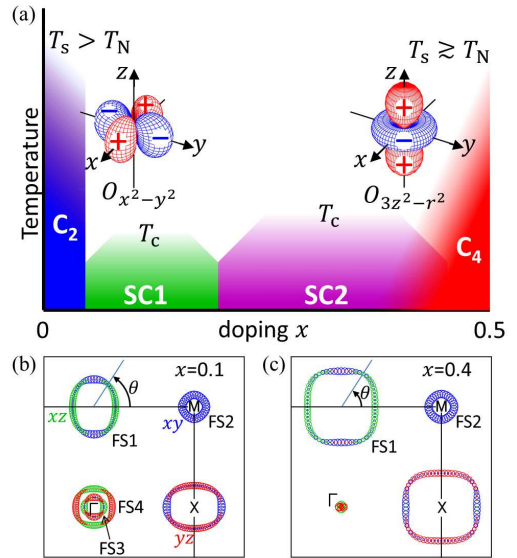


FIG. 1: (color online) (a) Schematic phase diagram of  $\text{LaFeAsO}_{1-x}\text{H}_x$ . We predict that non-nematic  $O_{3z^2-r^2}$  (nematic  $O_{x^2-y^2}$ ) charge quadrupole order emerges in the  $C_4$  ( $C_2$ ) phase. (b) FSs at  $x = 0.1$ , and (c) FSs at  $x = 0.4$  [21]. FS1 is electron-pocket, and FS2 (FS3,4) is hole-pocket composed of  $d_{xy}$  ( $d_{xz}, d_{yz}$ ) orbital.

In this paper, we study the overall phase diagram of  $\text{LaFeAsO}_{1-x}\text{H}_x$  ( $x = 0 \sim 0.5$ ) using the self-consistent vertex correction (SC-VC) method [5]. At  $x \sim 0$ , nematic orbital order ( $O_{x^2-y^2} = n_{xz} - n_{yz}$ ) is induced by the VC. At  $x \sim 0.5$ , in contrast, we obtain the non-nematic order ( $O_{3z^2-r^2} = \frac{1}{2}(n_{xz} + n_{yz}) - n_{xy}$ ) that couples to the

As-height change, consistently with the  $C_4$  isostructural transition for  $x > 0.45$ . We also improve the Migdal-Eliashberg theory by considering the VC for the gap equation, and find that the orbital-fluctuation-mediated  $s$ -wave state is stabilized by the VC. The present study reveals that multiple kinds of orbital fluctuations play significant roles in various Fe-based superconductors.

Figure 1 (a) shows the phase diagram of LaFeAsO $_{1-x}$ H $_x$ : We propose that the charge quadrupole order  $O_{3z^2-r^2}$  appears at  $x \sim 0.5$ , while  $O_{x^2-y^2}$  appears at  $x \sim 0$ . We stress that the softening of the longitudinal elastic modulus along the  $c$ -axis,  $C_{33}$ , is observed in under- and over-doped Ba(Fe $_{1-x}$ Co $_x$ ) $_2$ As $_2$  [20]. This fact indicates that the  $O_{3z^2-r^2}$  quadrupole fluctuations develop in various Fe-based compounds.

The tight-binding model of LaFeAsO $_{1-x}$ H $_x$  for  $0 \leq x \leq 0.5$  had been introduced in Ref. [13]. The Fermi surfaces (FSs) for  $x = 0.1$  and  $0.4$  are shown in Fig. 1 (b) and (c), respectively. The RPA analysis for this model had been performed in Refs. [21, 22]: At  $x \sim 0$ , the nesting between electron- and hole-FSs gives the magnetic fluctuations with  $\mathbf{Q} = (\pi, 0), (0, \pi)$ . At  $x = 0.4$ , electron-electron FS nesting gives the incommensurate fluctuations  $\mathbf{Q} \sim (\pi, \pi/3), (\pi/3, \pi)$ . Both the spin- and orbital-mediated  $s$ -wave states had been discussed in Ref. [21]. However, structure transition in under and over-doped regions cannot be explained by using the RPA.

Hereafter, we analyze the multiorbital Hubbard model with intra (inter) orbital interaction  $U$  ( $U'$ ) and the exchange interaction  $J$  using the SC-VC method. We put the constraint  $U = U' + 2J$ . It is found that strong ferro- and antiferro-quadrupole fluctuations are induced by the VC [5]. The charge (spin) susceptibility is given by

$$\chi_{l,l',m,m'}^{c(s)}(\mathbf{q}, \omega_l) = \int_0^\beta d\tau \langle A_{l,l'}^{c(s)}(\mathbf{q}, \tau) A_{m',m}^{c(s)}(-\mathbf{q}, 0) \rangle e^{i\omega_l \tau}$$

where  $A_{l,l'}^{c(s)}(\mathbf{q}) = \sum_{\mathbf{k}} (c_{l',\mathbf{k}\uparrow}^\dagger c_{l\mathbf{k}+\mathbf{q}\uparrow} + (-) c_{l',\mathbf{k}\downarrow}^\dagger c_{l\mathbf{k}+\mathbf{q}\downarrow})$ . Here,  $l, l', m, m'$  are  $d$  orbitals: We denote  $d_{3z^2-r^2}$ ,  $d_{xz}$ ,  $d_{yz}$ ,  $d_{xy}$ ,  $d_{x^2-y^2}$  orbitals as 1, 2, 3, 4, 5. The FSs are mainly composed of 2,3,4 orbitals.  $\hat{\chi}^{c(s)}(q)$  is given in the  $5^2 \times 5^2$  matrix form as

$$\hat{\chi}^{c(s)}(q) = \hat{\Phi}^{c(s)}(q) (1 - \hat{\Gamma}^{c(s)} \hat{\Phi}^{c(s)}(q))^{-1} \quad (1)$$

where  $q = (\mathbf{q}, \omega_l)$  and  $\hat{\Phi}^{c(s)}(q) = \hat{\chi}^{(0)}(q) + \hat{X}^{c(s)}(q)$ :  $\hat{\chi}^{(0)}(q)$  is the bare susceptibility and  $\hat{X}^{c(s)}(q)$  is the VC for charge (spin) channel.  $\hat{\Gamma}^{c(s)}$  is the matrix form of the bare Coulomb interaction for the charge (spin) sector [23]. In the original SC-VC method, the VC is given by the Maki-Thompson (MT) and Azlamasov-Larkin (AL) terms, which are the first and second order terms with respect to  $\hat{\chi}^{c,s}$ , respectively. Here, we put  $\hat{X}^s(q) = 0$ , and calculate only the AL term for  $\hat{X}^c(q)$  self-consistently. Its justification is shown in Refs. [24], and also confirmed by the recent renormalization group study [25].

We introduce the quadrupole susceptibilities as

$$\chi_\gamma^Q(\mathbf{q}, \omega_l) = \sum_{l,l',m,m'} O_\gamma^{l,l'} \chi_{l,l',m,m'}^c(\mathbf{q}, \omega_l) O_\gamma^{m',m}, \quad (2)$$

where  $\gamma = x^2 - y^2, 3z^2 - r^2, xz, yz, xy$ . The nonzero matrix elements of  $\hat{O}_\gamma$  with respect to 2  $\sim$  4 orbitals are  $O_{x^2-y^2}^{2,2} = -O_{x^2-y^2}^{3,3} = 1$ ,  $2O_{3z^2-r^2}^{2,2} = 2O_{3z^2-r^2}^{3,3} = -O_{3z^2-r^2}^{4,4} = 1$ , and  $O_{xz}^{3,4} = O_{xz}^{4,3} = 1$  [23]. Then,  $\chi_{x^2-y^2}^Q(q) \approx \chi_{2,2;2,2}^c(q) + \chi_{3,3;3,3}^c(q) - 2\chi_{2,2;3,3}^c(q)$ , and  $\chi_{3z^2-r^2}^Q(q) \approx \chi_{4,4;4,4}^c(q) - (\chi_{2,2;4,4}^c(q) + \chi_{3,3;4,4}^c(q)) + (\chi_{2,2;2,2}^c(q) + \chi_{3,3;3,3}^c(q) + 2\chi_{2,2;3,3}^c(q))/4$ .

Now, we study the tight-binding models of LaFeAsO $_{1-x}$ H $_x$  based on the SC-VC theory. In our previous SC-VC study [5], we have interested in the developments of  $\chi_{x^2-y^2}^Q(q)$  and  $\chi_{xz,yz}^Q(q)$ , so we have dropped  $X_{l,l';4,4}^c(q)$  (and  $X_{4,4;l,l}^c(q)$ ). In the present study, we include  $X_{l,l';4,4}^c(q)$ , and find that  $\chi_{3z^2-r^2}^Q(q)$  is also strongly enhanced due to large  $X_{4,4;4,4}^c(q)$ . In the numerical study, we fix the temperature at  $T = 0.05eV$ . Hereafter, the unit of energy is eV.

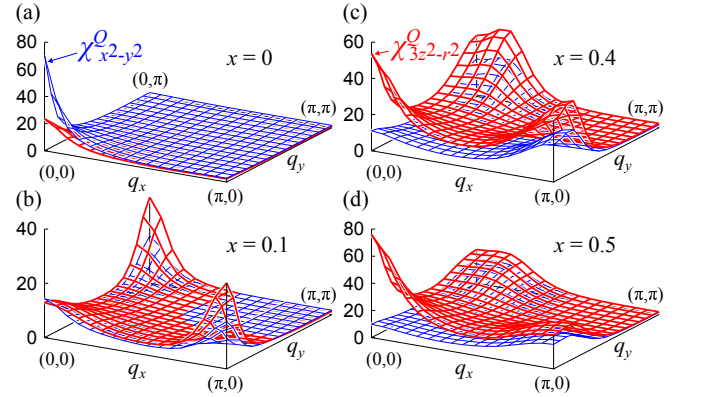


FIG. 2: (color online)  $\chi_{3z^2-r^2}^Q(q)$  (red lines) and  $\chi_{x^2-y^2}^Q(q)$  (blue lines) for (a)  $x = 0$  ( $U = 1.39$ ), (b)  $x = 0.1$  ( $U = 1.34$ ), (c)  $x = 0.4$  ( $U = 1.06$ ) and (d)  $x = 0.5$  ( $U = 0.99$ ), obtained by the SC-VC method. Stoner factors are  $\alpha_c = 0.97$  and  $\alpha_s \sim 0.9$ . In the SC-VC method,  $\chi_{xz/yz}^Q(q)$  is subdominant and not shown.

Figure 2 (a)-(d) shows the obtained  $\chi_{3z^2-r^2}^Q(q)$  and  $\chi_{x^2-y^2}^Q(q)$  under the constraint  $J/U = 0.055$ . For each  $x$ , we choose the value of  $U$  so that the charge Stoner factor satisfy  $\alpha_c = 0.97$ . Then, the realized spin Stoner factor is  $a_s \gtrsim 0.9$  for each  $x$ . Here,  $\alpha_{c(s)}$  is given by the maximum eigenvalue of  $\hat{\Gamma}^{c(s)} \hat{\Phi}^{c(s)}(q)$  in eq. (1), and  $\alpha_{c(s)} = 1$  corresponds to the quadrupole (spin) order. At  $x = 0$  in (a), the divergent peak of  $\chi_{x^2-y^2}^Q(\mathbf{0})$  corresponds to the  $C_2$  structure transition. In addition, large  $\chi_{3z^2-r^2}^Q(\mathbf{0})$  gives the softening of  $C_{33}$  reported in Ref. [20]. At  $x = 0.1$  in (b), which corresponds to the first  $T_c$  dome in Fig. 2, we obtain strong antiferro-quadrupole fluctuations for  $\gamma = x^2 - y^2$  and  $3z^2 - r^2$  channels. At  $x = 0.4$  in (c),

which corresponds to the second  $T_c$  dome, the quadrupole fluctuations become incommensurate, reflecting the bad nesting shown in Fig. 1 (c). Both for  $x \sim 0.1$  and  $x \sim 0.4$ , strong antiferro- and ferro-quadrupole fluctuations cause the  $s$ -wave state without sign reversal ( $s_{++}$ -wave state), as we will discuss later. At  $x = 0.5$  in (d), the divergent peak of  $\chi_{3z^2-r^2}^Q(\mathbf{0})$  gives the non-nematic ( $C_4$ ) orbital fluctuations and As-height instability.

The evidence for ferro-quadrupole fluctuations had been provided by the softening of the elastic constants  $C_{66}$  and  $C_{33}$ . According to Ref. [26], they are given as  $C_{66}^{-1} \propto 1 + g_{x^2-y^2}\chi_{x^2-y^2}^Q(0)$  and  $C_{33}^{-1} \propto 1 + g_{3z^2-r^2}\chi_{3z^2-r^2}^Q(0)$ , where  $g_\gamma$  is the quadrupole interaction for  $\gamma$ -channel due to the acoustic phonon [26]. Thus, the band Jahn-Teller effect due to acoustic phonon also contributes to the structure transition. However, it gives minor contribution in Fe-pnictides since the orthorhombicity  $(a-b)/(a+b)$  in the  $C_2$  phase is just  $\sim 0.3\%$  [26]. When  $g_{3z^2-r^2}$  is very small, the softening of  $C_{33}$  is not large even when  $\chi_{3z^2-r^2}^Q(0) \gg 1$ . In addition, we expect that the pseudo-gap in LaFeAsO $_{1-x}$ H $_x$  observed by photoemission [27] is given by the strong  $(\pi, 0)$  quadrupole fluctuations, and the nematic order at  $T^* > T_{S,N}$  [28, 29] is explained by the  $(\pi, 0)$  quadrupole order, which could be stabilized by impurity potentials [30].

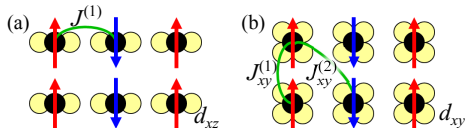


FIG. 3: (color online) (a) Localized ( $d_{xz}, d_{yz}$ )-orbital model with Kugel-Khomskii coupling. (b) Localized  $d_{xy}$ -orbital model with Heisenberg coupling.

Here, we try to understand the orbital-spin mode-coupling due to AL term in terms of the localized picture  $U \gg W_{\text{band}}$ : First, we introduce the Kugel-Khomskii type orbital-dependent exchange interaction with the nearest neighbor  $d_{xz}, d_{yz}$ -orbitals,  $H' \sim J^{(1)} \sum_{\langle i,j \rangle} (\mathbf{s}_i \cdot \mathbf{s}_j) (n_{xz}^i n_{xz}^j \delta_{i-j, (\pm 1, 0)} + n_{yz}^i n_{yz}^j \delta_{i-j, (0, \pm 1)})$ , as shown in Fig. 3 (a). Note that  $J^{(1)} \sim 2t^2/U$ . Due to this orbital-spin coupling term, if the AFM order with  $\mathbf{Q} = (\pi, 0)$  is realized, the electrons at each site will occupy the  $d_{xz}$ -orbital, as shown in Fig. 3 (a). That is, the AFM order or fluctuations induces the  $C_2$  orbital order ( $n_{xz} \neq n_{yz}$ ) or fluctuations, and vice versa. Next, we consider the single  $d_{xy}$ -orbital model with the nearest and next-nearest-neighbor exchange interactions:  $H'' \sim J_{xy}^{(1)} \sum_{\langle i,j \rangle} (\mathbf{s}_i \cdot \mathbf{s}_j) (n_{xy}^i n_{xy}^j) + J_{xy}^{(2)} \sum_{\langle\langle i,j \rangle\rangle} (\mathbf{s}_i \cdot \mathbf{s}_j) (n_{xy}^i n_{xy}^j)$ . When  $J_{xy}^{(2)} > \frac{1}{2} J_{xy}^{(1)}$ , the  $\mathbf{Q} = (\pi, 0)$  AFM state in Fig. 3 (b) appears due to “order-by-disorder” mechanism [31].

Now, we consider the three-orbital model  $H' + H''$ : When  $J_{xy}^{(2)} \gg J^{(1)}$ , the ferro-orbital order  $n_{xy} \gg n_{xz} = n_{yz}$  with AFM order shown in Fig. 3 (b) would be real-

ized to gain the exchange energy. In this case, the AFM order or fluctuations induces non-nematic  $C_4$  orbital order or fluctuations, and vice versa. This case corresponds to  $x \sim 0.5$  with strong  $d_{xy}$ -orbital spin fluctuations.

We also discuss why the VC induces the  $C_4$  ( $C_2$ ) order at  $x = 0.5$  ( $x = 0$ ) microscopically: When spin fluctuations develop mainly in the  $l$ -orbital, the charge AL-term  $X_{l,l;l,l}^c(\mathbf{0}) \sim T \sum_{\mathbf{k}} \{\chi_{l,l;l,l}^s(\mathbf{k})\}^2$  becomes large [5, 24]. Now, we analyze  $\chi_\gamma^Q(\mathbf{0})$  for  $J = 0$ , by inputting only three irreducible susceptibilities  $\Phi_l^c \equiv \chi_{l,l;l,l}^{(0)}(\mathbf{0}) + X_{l,l;l,l}^c(\mathbf{0})$  ( $l = 2 \sim 4$ ) into eq. (1). Then, we obtain [24]

$$\chi_{x^2-y^2}^Q(\mathbf{0}) = 2\Phi_2^c(1 - U\Phi_2^c)^{-1}, \quad (3)$$

$$\chi_{3z^2-r^2}^Q(\mathbf{0}) = b(1 - aU\Phi_4^c)^{-1}, \quad (4)$$

where  $a \equiv (5U\Phi_2^c - 1)/(3U\Phi_2^c + 1)$  and  $b \sim (5U\Phi_4^c + 1)^2/16U^2\Phi_4^c$  near the QCP. In the case of  $\Phi_2^c = \Phi_3^c > \Phi_4^c$ , then  $\chi_{x^2-y^2}^Q(\mathbf{0})$  is the most divergent. In the opposite case,  $\chi_{3z^2-r^2}^Q(\mathbf{0})$  is the most divergent if  $a$  is positive. At  $x \sim 0.5$ , two  $d_{xz}, d_{yz}$ -orbital FSs (FS3,4) disappear as shown in Fig. 1 (c), so  $d_{xy}$ -orbital spin fluctuations becomes dominant [21]. For this reason, at  $x \sim 0.5$ , the  $O_{3z^2-r^2}$  order and As-height instability are driven by  $\Phi_4^c$  due to strong  $d_{xy}$ -orbital spin fluctuations.

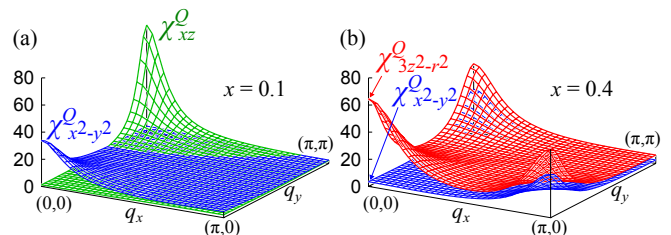


FIG. 4: (color online)  $\chi_{3z^2-r^2}^Q(q)$  (red lines),  $\chi_{x^2-y^2}^Q(q)$  (blue lines), and  $\chi_{xz}^Q(q)$  (green lines) for (a)  $x = 0.1$  ( $U = 2.0$ ) and (b)  $x = 0.4$  ( $U = 1.6$ ), obtained by the SC-VC $_\Sigma$  method in the case of  $J/U = 0.12$ . Stoner factors are  $\alpha_c = 0.97$  and  $\alpha_s \approx 0.9$ .

In the previous SC-VC study for  $x = 0.1$  [5], we obtained strong AF orbital fluctuations  $\chi_{xz}^Q(q) \approx 2\chi_{3,4;3,4}^c(q) + 2\chi_{3,4;4,3}^c(q)$  due to large AL-VC  $X_{3,4;3,4}^c$  and good inter-orbital nesting of the FS at  $\mathbf{q} \sim \mathbf{Q}$ . In the present SC-VC study, however, we obtain  $\chi_{3z^2-r^2}^Q \gg \chi_{xz}^Q$  since large  $X_{4,4;4,4}^c$  is induced by strong  $d_{xy}$ -orbital spin fluctuations. However,  $\chi_{3z^2-r^2}^Q$  in the present SC-VC might be over-estimated since the self-energy  $\Sigma$  is absent in the SC-VC method: In fact, large  $\Sigma$  due to  $d_{xy}$ -orbital spin fluctuations causes the negative feedback to suppress the fluctuations on the same orbital.

To consider the effect of  $\Sigma$ , we perform the “self-consistent VC+ $\Sigma$  (SC-VC $_\Sigma$ ) method”, in which we calculate both  $\hat{X}$  and  $\hat{\Sigma}$  self-consistently [32]. We include the AL terms  $A_{l,l;4,4}^c$ , and the obtained  $\chi_\gamma^Q(q)$  under the constraint  $J/U = 0.12$  are shown in Fig. 4. For  $x = 0.1$

in (a),  $\chi_{xz}^Q(\mathbf{Q})$  is strongly enlarged consistently with the report in Ref. [5]: By including the self-energy,  $\chi_{3z^2-r^2}^Q$  becomes small (not shown) since the  $d_{xy}$ -orbital spin fluctuations are suppressed. For  $x = 0.4$  in (b), on the other hand, we obtain strong ferro- and antiferro-quadrupole fluctuations for  $\gamma = 3z^2 - r^2$  channels, similarly to the results in Fig. 2 (c). Thus, the obtained results for  $x \sim 0.4$  are robust with respect to the self-energy correction.

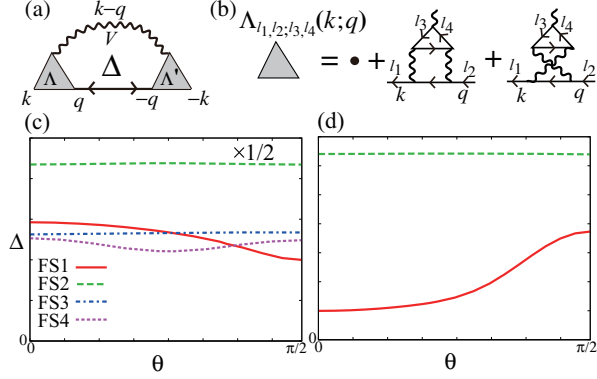


FIG. 5: (color online) (a) Gap equation with  $\Delta$ -VC and (b) AL-type diagram for  $\Lambda$ . The obtained  $s_{++}$ -wave gap functions on the FSs for (c)  $x = 0.1$  and (d)  $x = 0.4$  are shown.  $\theta$  is the azimuthal angle in Fig. 1 (c) and (d). Here,  $\Delta_{\text{FS2}}$  tends to be very large in both orbital- and spin-fluctuation studies, due to very small Fermi velocity of FS2 in the present model.

Next, we study the superconductivity due to orbital and spin fluctuations, based on the SC-VC $_{\Sigma}$  method. In almost all previous studies, the VC for the gap equation ( $\Delta$ -VC) had been dropped. In strongly correlated systems, however,  $\Delta$ -VC could be quantitatively important since the Migdal's theorem is not valid any more. Since the AL-type VC for  $\chi_{\gamma}^Q(q)$  is very large,  $\Delta$ -VC due to AL-type diagram should be significant. Here, we solve the following gap equation in the orbital-basis by taking the  $\Delta$ -VC into account:

$$\lambda_E \Delta_{l,l'}(k) = -T \sum_{q, m_i} V_{l, m_1; m_4, l'}(k, q) G_{m_1, m_2}(q) \times \Delta_{m_2, m_3}(q) G_{m_4, m_3}(-q) \quad (5)$$

where  $\lambda_E$  is the eigenvalue,  $\Delta_{l,l'}(k)$  is the gap function, and  $G_{l,l'}(q)$  is the Green function with self-energy. The pairing interaction  $V_{l, m_1; m_4, l'}(k, q)$  is given as

$$\hat{V}(k, q) = \frac{3}{2} \hat{\Lambda}^s(k, q) \hat{\Gamma}^s \hat{\chi}^s(k - q) \hat{\Gamma}^s \hat{\Lambda}^s(-k, -q) - \frac{1}{2} \hat{\Lambda}^c(k, q) \hat{\Gamma}^c \hat{\chi}^c(k - q) \hat{\Gamma}^c \hat{\Lambda}^c(-k, -q) + V^{(1)}(6)$$

where  $\hat{\Lambda}^{c(s)}(k, q)$  is the vertex for the charge (spin) channel shown in Fig. 5 (a),  $\Lambda_{l, l'; m, m'}^{c(s)}(k, q) = \Lambda_{m', m; l', l}^{c(s)}(k, q)$ , and  $V^{(1)} = \frac{1}{2}(\hat{\Gamma}^s - \hat{\Gamma}^c)$ . To make consistency with the SC-VC method, we calculate the AL-type contribution to  $\hat{\Lambda}^c(k, q)$  given in Fig. 5 (b), whereas we put  $\hat{\Lambda}^s(k, q) = \hat{1}$ .

Figure 5 shows the obtained superconducting gaps in the band-basis for (c)  $x = 0.1$  and (d)  $x = 0.4$ . In both cases, the  $s_{++}$ -state is realized by taking the  $\Delta$ -VC into account beyond the Migdal's theorem, since the attractive interaction due to  $\hat{\chi}^c$  in eq. (6) is multiplied by  $|\hat{\Lambda}^c(k, q)|^2 \gg 1$  as discussed in Refs [5, 32]. (If we drop  $\Delta$ -VC as usual, then  $s_{\pm}$ -state is favored because of the factor 3 for the spin channel in eq. (6).) The  $s_{++}$  state is realized against the strong Coulomb repulsion due to the retardation effect, since the energy-scale of orbital fluctuations is much smaller than  $W_{\text{band}}$  near the orbital QCP. The obtained  $s_{++}$  state is consistent with the robustness of  $T_c$  against the randomness in Fe-pnictides [36, 39, 40].

In summary, the overall phase diagram of  $\text{LaFeAsO}_{1-x}\text{H}_x$  ( $x = 0 \sim 0.5$ ) are well reproduced using the orbital fluctuation theory. We predicted that the non-nematic  $O_{3z^2-r^2}$  order is the origin of the new  $C_4$  isostructural transition at  $x \sim 0.5$  [13]. At  $x \sim 0$ , ferro- $O_{x^2-y^2}$  order triggers the  $C_2$  transition. We obtain the orbital-fluctuation-mediated  $s_{++}$ -wave state for both  $x \sim 0.1$  and  $x \sim 0.4$ , by including the VC for the gap equation ( $\Delta$ -VC). The switch of the dominant quadrupole fluctuations in Fig. 2 will be the origin of the double-dome structure of  $T_c$ . This new class of superconductivity due to non-nematic orbital fluctuations would be realized in other compounds, like Pr-doped and (La,P)-doped  $\text{CaFe}_2\text{As}_2$ .

We are grateful to H. Hosono, J. Yamaura, Y. Murakami, N. Fujiwara, H. Hiraga and S. Iimura for useful discussions. This study has been supported by Grants-in-Aid for Scientific Research from MEXT of Japan.

- 
- [1] Y. Mizuguchi and Y. Takano, J. Phys. Soc. Jpn. **79**, 102001 (2010).
  - [2] R. M. Fernandes, L. H. VanBebber, S. Bhattacharya, P. Chandra, V. Keppens, D. Mandrus, M. A. McGuire, B. C. Sales, A. S. Sefat, and J. Schmalian, Phys. Rev. Lett. **105**, 157003 (2010).
  - [3] W. Lv, F. Krüger, and P. Phillips, Phys. Rev. B **82**, 045125 (2010).
  - [4] C.-C. Lee, W.-G. Yin, and W. Ku, Phys. Rev. Lett. **103**, 267001 (2009).
  - [5] S. Onari and H. Kontani, Phys. Rev. Lett. **109**, 137001 (2012).
  - [6] S. Liang, A. Moreo, and E. Dagotto, arXiv:1305.1879.
  - [7] M. Yoshizawa, D. Kimura, T. Chiba, S. Simayi, Y. Nakanishi, K. Kihou, C.-H. Lee, A. Iyo, H. Eisaki, M. Nakajima, and S. Uchida, J. Phys. Soc. Jpn. **81**, 024604 (2012).
  - [8] A. E. Böhrer, P. Burger, F. Hardy, T. Wolf, P. Schweiss, R. Fromknecht, M. Reinecker, W. Schranz, and C. Meingast, arXiv:1305.3515
  - [9] M. Yi, D. Lu, J.-H. Chu, J. G. Analytis, A. P. Sorini, A. F. Kemper, B. Moritz, S.-K. Mo, R. G. Moore, M. Hashimoto, W.-S. Lee, Z. Hussain, T. P. Devereaux, I. R. Fisher, and Z.-X. Shen, Proc. Natl. Acad. Sci. USA

- 108**, 6878 (2011).
- [10] T. Shimojima, T. Sonobe, W. Malaeb, K. Shinada, A. Chainani, S. Shin, T. Yoshida, S. Ideta, A. Fujimori, H. Kumigashira, K. Ono, Y. Nakashima, H. Anzai, M. Arita, A. Ino, H. Namatame, M. Taniguchi, M. Nakajima, S. Uchida, Y. Tomioka, T. Ito, K. Kihou, C. H. Lee, A. Iyo, H. Eisaki, K. Ohgushi, S. Kasahara, T. Terashima, H. Ikeda, T. Shibauchi, Y. Matsuda, and K. Ishizaka, arXiv:1305.3875
- [11] Y. Gallais, R. M. Fernandes, I. Paul, L. Chauviere, Y.-X. Yang, M.-A. Measson, M. Cazayous, A. Sacuto, D. Colson, and A. Forget, arXiv:1302.6255
- [12] H. Kontani and Y. Yamakawa, unpublished.
- [13] S. Iimura, S. Matuishi, H. Sato, T. Hanna, Y. Muraba, S. W. Kim, J. E. Kim, M. Takata, and H. Hosono, Nat. Commun. **3**, 943 (2012).
- [14] N. Fujiwara, S. Tsutsumi, S. Iimura, S. Matsuishi, H. Hosono, Y. Yamakawa, and H. Kontani, Phys. Rev. Lett. **111**, 097002 (2013).
- [15] H. Hosono, J. Yamaura, Y. Murakami, H. Hiraga and S. Iimura, private communication.
- [16] For  $x > 0.5$ , in addition to the  $c$ -axis length change, Fe-layers and As-layers slide alternatively at  $T_S$  [15]. The latter may be due to band-JT effect since the lattice deformation is very large.
- [17] S. R. Saha, N. P. Butch, T. Drye, J. Magill, S. Ziemak, K. Kirshenbaum, P. Y. Zavaliy, J. W. Lynn, and J. Paglione, Phys. Rev. B **85**, 024525 (2012).
- [18] K. Kudo, K. Iba, M. Takasuga, Y. Kitahama, J. Matsumura, M. Danura, Y. Nogami, and M. Nohara, Sci. Rep. **3**, 1478 (2013).
- [19] S. Simayi, K. Sakano, H. Takezawa, M. Nakamura, Y. Nakanishi, K. Kihou, M. Nakajima, C.-H. Lee, A. Iyo, H. Eisaki, S. Uchida, and M. Yoshizawa, J. Phys. Soc. Jpn. **82**, 114604 (2013).
- [20] S. Simayi, K. Sakano, H. Takezawa, M. Nakamura, Y. Nakanishi, K. Kihou, M. Nakajima, C. Lee, A. Iyo, H. Eisaki, S. Uchida, and M. Yoshizawa, arXiv:1310.2681
- [21] Y. Yamakawa, S. Onari, H. Kontani, N. Fujiwara, S. Iimura, and H. Hosono, Phys. Rev. B **88**, 041106(R) (2013).
- [22] K. Suzuki, H. Usui, K. Kuroki, S. Iimura, Y. Sato, S. Matsuishi, and H. Hosono, J. Phys. Soc. Jpn. **82**, 083702 (2013).
- [23] H. Kontani and S. Onari, Phys. Rev. Lett. **104**, 157001 (2010).
- [24] Y. Ohno, M. Tsuchiizu, S. Onari, and H. Kontani, J. Phys. Soc. Jpn **82**, 013707 (2013).
- [25] M. Tsuchiizu, Y. Ohno, S. Onari, and H. Kontani, Phys. Rev. Lett. **111**, 057003 (2013).
- [26] H. Kontani, T. Saito, and S. Onari, Phys. Rev. B **84**, 024528 (2011).
- [27] A. Nakamura, T. Shimojima *et al.*, private communication.
- [28] S. Kasahara, H. J. Shi, K. Hashimoto, S. Tonegawa, Y. Mizukami, T. Shibauchi, K. Sugimoto, T. Fukuda, T. Terashima, A. H. Nevidomskyy, and Y. Matsuda, Nature **486**, 382 (2012).
- [29] Y. K. Kim, W. S. Jung, G. R. Han, K.-Y. Choi, K.-H. Kim, C.-C. Chen, T. P. Devereaux, A. Chainani, J. Miyawaki, Y. Takata, Y. Tanaka, M. Oura, S. Shin, A. P. Singh, H. G. Lee, J.-Y. Kim, and C. Kim, Phys. Rev. Lett. **111**, 217001 (2013).
- [30] H. Kontani, Y. Inoue, T. Saito, Y. Yamakawa, and S. Onari, Solid State Commun. **152**, 718 (2012).
- [31] E. Shender, Sov. Phys. JETP **56**, 178 (1982); C. L. Henley, Phys. Rev. Lett. **62**, 2056 (1989); A. Moreo, E. Dagotto, T. Jolicur and J. Riera, Phys. Rev. B **42**, 6283 (1990); P. Chandra, P. Coleman, and A. Larkin, Phys. Rev. Lett. **64**, 88 (1990).
- [32] S. Onari, H. Kontani, S. V. Borisenko, V. B. Zabolotnyy, and B. Buechner, arXiv:1307.6119
- [33] K. Kuroki, S. Onari, R. Arita, H. Usui, Y. Tanaka, H. Kontani, and H. Aoki, Phys. Rev. Lett. **101**, 087004 (2008).
- [34] P. J. Hirschfeld, M. M. Korshunov, and I. I. Mazin, Rep. Prog. Phys. **74**, 124508 (2011).
- [35] A. V. Chubukov, D. V. Efremov, and I. Eremin, Phys. Rev. B **78**, 134512 (2008).
- [36] A. Kawabata, S. C. Lee, T. Moyoshi, Y. Kobayashi, and M. Sato, J. Phys. Soc. Jpn. **77**, 103704 (2008).
- [37] Y. Nakajima, T. Taen, Y. Tsuchiya, T. Tamegai, H. Kitamura, and T. Murakami, Phys. Rev. B **82**, 220504 (2010).
- [38] J. Li, Y. Guo, S. Zhang, J. Yuan, Y. Tsujimoto, X. Wang, C.I. Sathish, Y. Sun, S. Yu, W. Yi, K. Yamaura, E. Takayama-Muromachi, Y. Shirako, M. Akaogi, and H. Kontani, Phys. Rev. B **85**, 214509 (2012).
- [39] S. Onari and H. Kontani, Phys. Rev. Lett. **103**, 177001 (2009).
- [40] Y. Yamakawa, S. Onari, and H. Kontani, Phys. Rev. B **87**, 195121 (2013).